THE VOICE OF THE DRAGON: A PHYSICAL MODEL OF A ROTATING CORRUGATED TUBE

Stefania Serafin

CCRMA, Department of Music
Stanford University
serafin@ccrma.stanford.edu

Juraj Kojs

McIntire Department of Music
University of Virginia
jk6ax@virginia.edu

ABSTRACT

When an unsmooth flexible tube rotates, rich tones are produced. We propose a physical model that simulates this behavior. The tube is modeled as an open-ended organ pipe blown by an air stream pumped by a rotationally induced pressure which follows Bernoulli's principle.

1. INTRODUCTION

The *Voice of the dragon* is the name given to a group of Japanese children twirling flexible plastic tubes above their heads. The burst of tones that emerged from each musical pipe soared and dropped with rotational velocity. A corrugated plastic tube, infact, produces pleasant sonorities while rotating in a circular motion.

Singing corrugated tubes became popular in early 70s when a toy called *hummer* was introduced to the market. The hummer is a corrugated plastic tube about one meter long, similar to the one shown in figure 1. When whirled in the air, the tube produces a series of pitches, starting from the first harmonic to its overtones. Mark Silvermann, after a visit to Japan where he heard

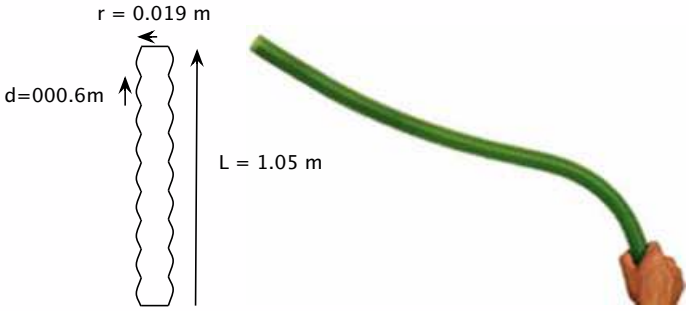

Figure 1: *A singing plastic tube and its relevant physical dimensions.*

the Japanese children's performance, studied the acoustics of such tubes [1]. He mounted the corrugated tube to a thin slab attached to a wheel free to rotate in a vertical plane, with a counterweight fixed at the opposite end of the slab so that the center of mass of the system laid on the axis of the wheel, as shown in figure 2. A motor whose velocity was varied using a rheostat was moving the wheel. Using a microphone, a stroboscope and a counter, the tones produced were recorded and the spin rates measured. The data were analyzed by Fourier analysis.

Also Crawford studied the acoustics of corrugated tube using a different device [2]. He attached the tube to his car and took it for a ride. Different tones were produced according to the car's velocity.

Both researchers made the following observations: whirling the tube slowly initiates the first overtone; with increased velocity, the higher partials resonate. Obviously, the length of the tube determines the pitches that will sing. Blowing into a smooth tube or whirl it in the air, no sound is produced. However, whirling a corrugated tube results in a noticeable tone. In a corrugated tube open at both ends, a tone is produced when the "bump" frequency of the air flowing through the tube equals one of the resonant frequencies of the tube. Air velocity, tube length, corrugation and diameter sizes therefore influence the pitch and volume of the sound produced.

The interest of toy makers as well as composers on singing tubes is due to the fact that the tubes' pure tones create an unusual ear-pleasing sonic zone easily discernible from the sound of the other bore-based instrument family members.

In the following section the sound production mechanism of corrugated tubes is described in details.

2. ACOUSTICS OF CORRUGATED TUBES

In order to understand how the corrugated tube produces sound, different components need to be taken into account.

For an ideal open-ended tube, the modes are given by the following expression:

$$f_n = \frac{nc}{2L} \tag{1}$$

for $n = 1, 2, 3, ..,$ where c is the speed of sound and L is the tube length [3]. Since the air is moving in an out of the tube, the effective length L' of the resonating column of air is actually given by [3]:

$$L' = L = 1.22r \tag{2}$$

where r is the radius of the tube.

As suggested in [1] and [2], with both ends open the tube resembles a centrifugal pump. When whirling, the air is sucked in through the end closer to the hand and pushed out through the outer end. In order to make the vibrational modes resonate and thus produce pitch, some of the airflow energy is converted to excitation energy.

It is interesting to investigate the dynamics of the tube first at a large scale and then at a microscale, which implies examining the role of the corrugations.

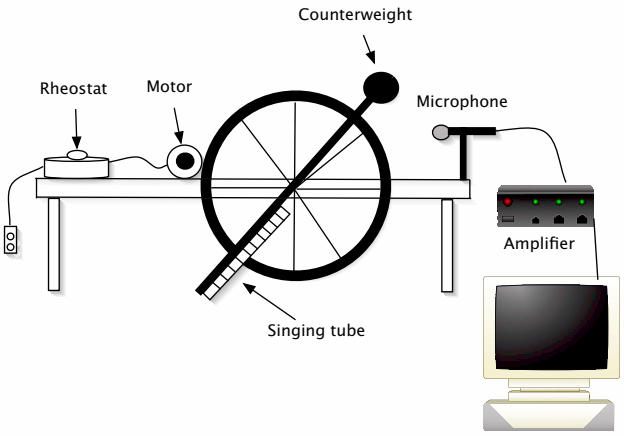

Figure 2: *The apparatus used in [1] to measure tube's frequencies and rotational velocity*

At a large scale there exists a vortical flow centered in the stationary end of the tube and normal to the axis of the tube with tangential air velocity given by:

$$V(s) = \omega_m s$$

where ω_m is the angular velocity and s is the position along the tube (from 0 to L).

Along the tube, the rotationally induced pressure difference between the two ends produces an axial flow with velocity v.

In order to relate the angular velocity ω_m to the pressure difference p, assuming the flow to be incompressible and smooth, we can use Bernoulli's principle:

$$p(s) + \frac{1}{2}\rho[v(s)^2 + \omega_m^2 s^2] = const. \tag{3}$$

where $p(s)$ is the pressure and $v(s)$ is the axial velocity at position s. With the same assumptions, the axial velocity through the tube is uniform, i.e. $v(s) = const.$ for $0 \leq s \leq L$. Therefore the pressure difference between the two extremities of the tube (stationary = 0 and rotating = L) is given by:

$$p = p(0) - p(L) = L^2\omega_m^2/2$$

It is now necessary to explain the role of the corrugations. This is done by relating axial air velocity v_n to distance between corrugations d as follows:

$$f_n = \alpha_1 \frac{v_n}{d} \tag{4}$$

where α_1 is a proportionality constant, v_n is the axial air velocity of mode n and f_n is the resonant frequency of that same mode. Equation 4 is justified by the fact that moving past the corrugations the air is perturbed at a frequency proportional to the axial air velocity and inversely proportional to the corrugation spacing. When f_n coincides with a resonant frequency of the tube, the sound is amplified.

We still need to relate the axial velocity v to the tangential air velocity $V(s)$. This is done by applying Bernoulli's equation 3 which gives $v_n = \omega_{mn} L = V(L)$, where ω_{mn} is the angular velocity of mode n. This equation states that, in case of frictionless flow, the axial velocity along the tube is the same as the tangential velocity at the rotating end. However, since the flow is not perfectly frictionless, we assume that the axial air velocity is proportional to the tangential air velocity:

$$v_n = \alpha_2 \omega_{mn} L \tag{5}$$

where α_2 is another proportionality constant (experimentally, however, $b = 1$ [1]). Combining equation 4 and 5 we obtain:

$$f_n = \alpha_1 \alpha_2 \frac{\omega_{mn} L}{d} \tag{6}$$

which states that the modes of the rotating tube are directly proportional to the angular velocity and inversely proportional to the distance between corrugations.

2.1. Accounting for friction

As previously mentioned, the flow inside the tube is not perfectly frictionless. Friction along the walls acts to resist the acceleration of air in the tube.

It can be shown [2] that friction generates a nonuniform flow and the effect of friction is to give $\alpha_1 = 2$. From equation 4 we can therefore conclude that $f_n = 2v_n/d$.

The previous equation states that knowing the axial air speed and the distance between corrugations, it is possible to calculate the frequency at which the tube resonate.

2.2. The Doppler effect

The finally component of the acoustics of the tube that influences its sonorities is the role of the rotation. When the tube rotates a *Doppler shift* is perceived, i.e. an apparent change in frequency content which is due to the motion of the tube relative to the listener. As derived in most elementary physics texts, the *Doppler shift* is given by

$$\omega_l = \omega_s \frac{1 + \frac{v_{ls}}{c}}{1 - \frac{v_{sl}}{c}} \tag{7}$$

where ω_s is the radian frequency emitted by the source at rest, ω_l is the frequency received by the listener, v_{ls} denotes the *speed* of the listener in the direction of the source, v_{sl} denotes the speed of the source in the direction of the listener, and c denotes sound speed.

3. ANALYSIS OF A CORRUGATED TUBE

We analyzed the tube shown in figure 1, in order to validate the theory presented in the previous section. The corrugated plastic tube was 1.08 m long, and with a radius $r = 0.019$ m. The corrugations were 6 mm long.

The second column of table 1 shows the theoretical modes of our corrugated tube, obtained using equation 1 with the radius correction proposed by Benade (see equation 2).

The third column shows the experimental frequencies obtained by recording the tube while rotating at different velocities and analyzing the amplitude of its frequency response. The peak of the spectrum were easily detected, since one strong mode is always perceivable. Note the good agreement between the experimental and theoretical frequency. The fourth column shows the rotational velocities associated with each frequencies. Those velocities were calculated looking at the time domain waveform, and counting the number of rotations per second which are clearly visible as, for

Mode number n	Theoretical Frequency	Experimental Frequency	Rotational Velocity
1	156 Hz		
2	312 Hz	$310Hz$	0.5 Hz
3	468 Hz	$464Hz$	0.9 Hz
4	624 Hz	$625Hz$	1.7 Hz
5	781 Hz	$769Hz$	2.5 Hz
6	937 Hz	$925Hz$	3.0 Hz
7	1093 Hz	$1081Hz$	3.3 Hz
8	1249 Hz	$1250Hz$	4.2 Hz

Table 1: *Mode number, theoretical and experimental frequency and rotational velocity of the tube used for the simulations.*

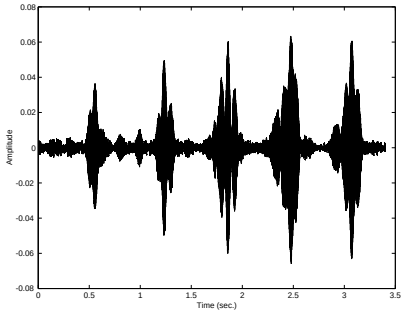

Figure 3: *Time domain waveforms for the corrugated tube when rotating at* 1.7 *rot/sec. Notice the modulations given by the Doppler effect.*

example, figure 3 shows. Each rotation, infact, corresponds to a modulation of the time domain waveform.

Figure 5 shows the amplitude of the frequency response for six modes of the tube. From top to bottom, mode 3, 4, 5, 6, 7 and 8 of the tube are shown (see table 1). Notice how a strong resonance is presence corresponding to each mean value of the rotational speed. While the rotational spedd is not discretized, the resonance frequencies are since they correspond to the resonant frequencies of the open-ended tube.

As a last analysis example, figure 5 shows the sonogram of the rotating tube while performing two arpeggios varying the rotational speed twice over time. High partials are amplified when the rotational speed increases, according to 1.

4. MODELING CORRUGATED TUBES

4.1. Waveguide model of a cylindrical tube

We consider the tube as an organ pipe open at both ends. A one dimensional digital waveguide such as the one shown in figure 6 can therefore be used to model the tube resonator [4]. Propagation losses are modeled using the bandpass filter $H_b(z)$ described in the following section.

4.2. Modeling the corrugations

We model the corrugations by reproducing their effect rather than building a precise physical model, since the turbulence inside the rotating tube are complex and still not well understood. The effect,

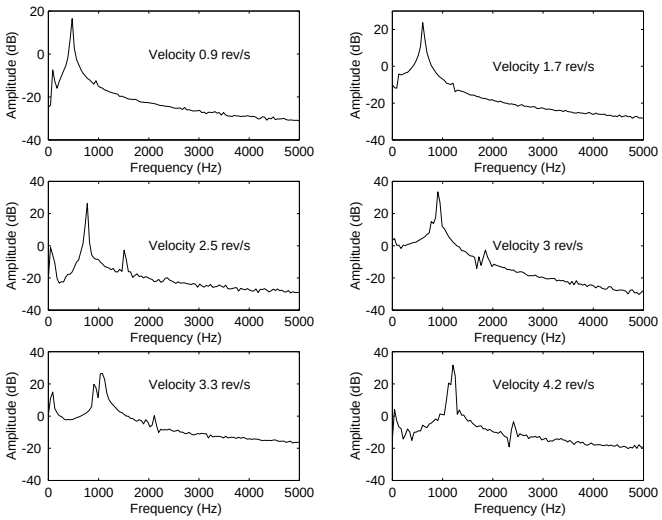

Figure 4: *Frequency response of six modes of the corrugated tube used for the simulations. The data correspond from top to bottom to frequencies and rotational velocity reported in table 1.*

on the other end, is rather clear and has already been explained by equation 4.

In our algorithm the distance between corrugations is known, and the axial air velocity v_n of mode n is calculated from equation 5, in which the rotational velocity is an input parameter of the model. At each sample i, we calculate the frequency f_{cn} for which $f_{cn} = v_n/d$, using equation 4. Then we calculate the closest mode f_a of the tube that corresponds to f_{cn}. This is the center frequency of a bandpass resonant filter whose role is to amplify f_a.

The simple algorithm to calculate the effect of corrugations is therefore the following:

```
known variables:  f_n, d, ω_m, L
for    i = 1... samples
       1) Compute    v_n from v_n = ω_mn L
       2) Compute    f_cn = v_n/d
       3) f_a = round(f_cn/f_0) f_0
          end
end
```

4.3. Modeling the Doppler effect

The last step of the tube simulation consists of modeling the rotation. The motion of the tube relative to the listener produces the well-known Doppler effect, i.e. an apparent change in frequency content of an acoustic signal. A simulation of the Doppler shift was proposed in [5] and [6].

Recently [7] a detailed simulation of the Doppler shift was proposed, which uses time varying delay lines [8]. The Doppler shift was applied to the simulation of the circular rotation of a Leslie horn.

Since there is a strong similarity between the rotation of the Leslie horn and the rotation of the corrugated tube, we use the same algorithm here. A more detailed derivation of the Doppler effect applied to a rotational source is found in [7].

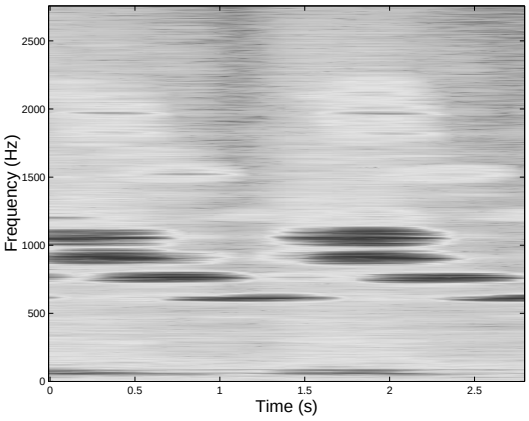

Figure 5: *Sonogram of the rotating tube while varying the rotational speed. Two arpeggios are obtained by varying the rotational speed.*

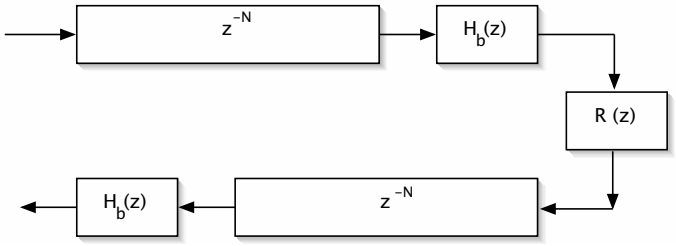

Figure 6: *Waveguide model of a cylindrical tube. Losses are lumped in the filters H_b. R represents a reflection filter.*

For a circularly rotating tube, the source position can be approximated as

$$\underline{x}_s(t) = \begin{bmatrix} r_s \cos(\omega_m t) \\ r_s \sin(\omega_m t) \end{bmatrix} \tag{8}$$

where r_s is the circular radius and ω_m is, as before, the angular velocity.

By (8), the source velocity for the circularly rotating tube is

$$\underline{v}_s(t) = \frac{d}{dt}\underline{x}_s(t) = \begin{bmatrix} -r_s\omega_m \sin(\omega_m t) \\ r_s\omega_m \cos(\omega_m t) \end{bmatrix} \tag{9}$$

Since the Doppler effect depends only on the relative position between the source and the listener [9], after some derivations that can be found in [7], we obtain:

$$\underline{v}_{sl} = \frac{-r_l r_s \omega_m \sin(\omega_m t)}{r_l^2 + 2 r_l r_s \cos(\omega_m t) + r_s^2} \begin{bmatrix} r_l - r_s \cos(\omega_m t) \\ -r_s \sin(\omega_m) t \end{bmatrix}. \tag{10}$$

where $\underline{v}_{sl}$ is the projected source velocity and r_l is the listener's radius. In the far field, this reduces simply to

$$\underline{v}_{sl} \approx -r_s\omega_m \sin(\omega_m t) \begin{bmatrix} 1 \\ 0 \end{bmatrix} \tag{11}$$

Substituting into the Doppler expression (7) with the listener velocity v_l set to zero yields

$$\omega_l = \frac{\omega_s}{1 + r_s\omega_m \sin(\omega_m t)/c} \approx \omega_s \left[1 - \frac{r_s\omega_m}{c} \sin(\omega_m t)\right], \tag{12}$$

where the approximation is valid for small Doppler shifts. Thus, in the far field, a rotating tube causes an approximately *sinusoidal* multiplicative frequency shift, with the amplitude given by tube's rotational radius r_s times tube angular velocity ω_m divided by sound velocity c.

5. THE COMPLETE MODEL

The complete singing tube model is summarized in figure 7.

The model is driven by two kinds of parameters:

1. **Physical parameters:** Length of the tube L and distance between corrugations d.
2. **Control parameters:** Angular velocity ω_m and rotational radius r_s.

The angular velocity ω_m and the rotational radius r_s are used as a parameter for the Doppler effect simulation. A fractional delay line [8] allows to continuously vary the discrete length N of the tube, where $N = f_s 2L/c$, where f_s is the sampling rate and c is, as before, the speed of sound in air.

A sharp second order resonant filter, tuned to the mode of the tube closest to $\omega_m L/d$, where d is the distance between corrugations, models the effect of corrugations as well as propagation losses.

We noticed, infact, that adding an additional lowpass filter to account for propagation losses along the tube does not improve the quality of the synthesis. We therefore lump all frequency dependent losses into the bandpass filter that accounts for corrugations.

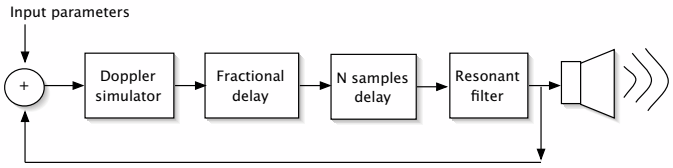

Figure 7: *Simplified block diagram of the complete model that simulates the corrugated tube.*

6. SIMULATION RESULTS

Figure 8 shows the sonogram of the synthetic corrugated tube while increasing the rotational speed. Notice how, as in the case of the real tube, one strong mode appears in the spectrum when the rotational speed increases.

7. MUSICAL APPLICATIONS

The corrugated tube's model has been implemented as an extension to the real-time environment Max/MSP [10]. The model of the singing tube has been used in the piece *Garden of Dragon* for cellophane, corrugated tubes and computer. This piece presents a communication between the virtual and real singing pipes using

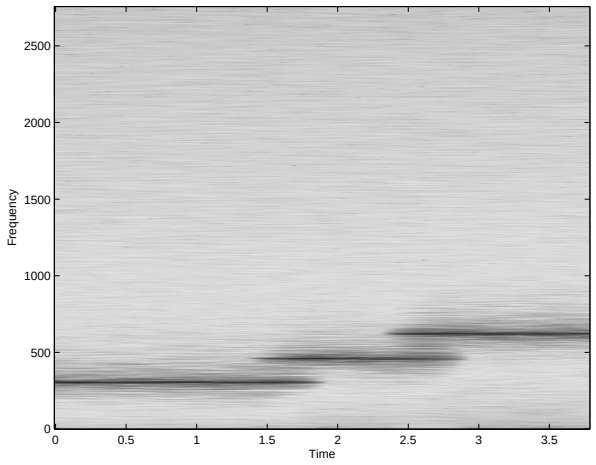

Figure 8: *Sonogram of the synthetic corrugated tube while increasing the rotational speed.*

Max/MSP. The Max/MSP physical model extends the possibilities of the real tubes in several areas: vibrato, pitch and amplitude control, and noise to pitch ratio. The acoustic tubes control the virtual choir of tubes using the fiddle∼ pitch tracker [11] of Max/MSP.

8. CONCLUSIONS

We proposed a model of a rotating corrugated tube which runs in real-time under the Max/MSP platform. The tube used in the experiments was the one that produced the most amplified and interesting sonorities compared to other corrugated tubes of different materials. From empirical observations we can state that the best sounding tubes are the ones with the most flexible shapes. Corrugations need to be interior to the tube, otherwise their effect disappears. Of course the symmetry of the tube is also important: corrugations placed at symmetrical positions along the tube produce nice sonorities, while tubes whose shape gets damaged after a long use become less resonant than newly produced tubes.

It is also interesting to notice that in vision there exists a phenomenon similar to the acoustical amplification that appears in the corrugated tubes called the Smith and Purcell radiation [12]: when an electron beam passes over a grating, it generates an oscillating image charge that radiates.

9. REFERENCES

[1] M. P. Silverman, "Voice of the Dragon: the rotating corrugated resonator," *Eur. J. Physics*, vol. 10, pp. 298–304, 1989.

[2] F.S. Crawford, "Singing Corrugated Pipes," *American Journal of Physics*, vol. 42, pp. 278–288, april 1974.

[3] A. Benade, *Fundamentals of Musical Acoustics*, Oxford University Press, 1976.

[4] Julius O. Smith III, "Physical Modeling using digital waveguides," *Computer Music Journal*, vol. 2, pp. 44–56, 1996.

[5] T. Takala and J. Hahn, "Sound rendering," *Computer Graphics*, vol. SIGGRAPH'92, no. 26, pp. 211–220, 1992.

[6] L. Savioja, J. Huopaniemi, T. Lokki, and R. Väänänen, "Creating interactive virtual acoustic environments," *Journal of the Audio Engineering Society*, vol. 47, no. 9, pp. 675–705, Sept. 1999.

[7] J.O. Smith, S. Serafin, J. Abel, and D. Berners, "Doppler Simulation and the Leslie," in *Proc. Workshop on Digital Audio Effects (DAFx-02)*, Hamburg, Germany, 2002, pp. 188–191.

[8] T. I. Laakso, V. Välimäki, M. Karjalainen, and U. K. Laine, "Splitting the Unit Delay—Tools for Fractional Delay Filter Design," *IEEE Signal Processing Magazine*, vol. 13, no. 1, pp. 30–60, January 1996.

[9] Allan D. Pierce, *Acoustics*, American Institute of Physics, for the Acoustical Society of America, (516)349-7800 x 481, 1989.

[10] D. Zicarelli, "An extensible real-time signal processing environment for MAX," in *Proc. International Computer Music Conference*, Michigan, Ann Arbour, 1998, pp. 463–466.

[11] M. Puckette and T. Apel, "Real time audio analysis tools for Pd and Max/MSP," in *Proc. International Computer Music Conference*, Michigan, Ann Arbour, 1998, pp. 109–112.

[12] S.J. Smith and M. Purcell, "Visible light from Localized Surface Charges moving across a grating," *Physics Review*, vol. 92, pp. 1069, 1953.